



## AN ELEMENTARY THEORY OF ONE-DIMENSIONAL ROD PENETRATION USING A NEW ESTIMATE FOR PRESSURE

P. WANG and S. E. JONES

Department of Engineering Science and Mechanics, The University of Alabama, Tuscaloosa,  
AL 35487, U.S.A.

(Received 20 April 1994; in revised form 28 March 1995)

**Summary**—In this paper, a new pressure law is proposed to replace the modified Bernoulli equation of Tate in 1967 and 1969. It is achieved by decomposing the equation of motion, which was proposed by Jones *et al.* in 1987, into two parts and incorporating the kinematic equation by Wilson *et al.* in 1989. The new pressure law takes the effect of mushroom strain into account. From two different considerations, the pressure law is applied to the one-dimensional penetration modeling. First, by assuming that the rod/target interface pressure is approximately constant during the quasi-steady state, the governing equations can be analytically integrated to give a closed form solution for the penetration depth. The prediction is reasonably good in the low velocity regime. Secondly, a velocity-dependent interface pressure is added. A so-called shape factor, which was first introduced without physical interpretation by Alekseevskii in 1966, is substantiated. With this factor, the governing equations can be numerically integrated to give very accurate predictions for the impact velocity range from 1 km/s to 4 km/s.

### INTRODUCTION

In the model developed by Alekseevskii [1] and Tate [2], the behavior of the rod is assumed to have two consecutive deformation zones. The first zone is a wafer thin plastic region, which is instantaneously eroded at the tip (or rod/target interface) of the rod. The second zone is the current uneroded (rigid) portion of the rod. In the first zone, the rod material is assumed to behave hydrodynamically, and in the second zone the rod is rigid over its uneroded length. The transition between these two zones is assumed to occur somewhere around the maximum stress (ultimate dynamic yield strength) that the rod can sustain as a rigid body. Beyond this dynamic yield strength, the material then behaves more like an incompressible and inviscid fluid in steady state. In order to simulate this transition phenomenon, for the first zone, they introduced the modified Bernoulli equation, which includes both dynamic strengths of the rod and target. This was used to estimate the rod/target interface pressure and to relate the current penetration velocity to the current velocity of the uneroded rod. As to the second zone, they applied Newton's second law to estimate a decelerated motion for the undeformed section. However, a factor that is controversial, but vital to the modified Bernoulli equation, is how to determine the strengths for the rod and target materials. These strength values are frequently obtained by matching the theoretical prediction of penetration depth with experimental data. A variety of attempts to estimate the target strength analytically thus became the focus of many efforts in verifying or revising the theory of Tate and Alekseevskii. Tate [3, 4] developed a flow field model, from which the modified Bernoulli equation was derived and the strength factors were correlated to material constants. Assuming elastic-plastic behavior of the rod and target material, the size of plastic region in the rod was estimated. It was suggested by Tate that a treatment of the unsteady motion could be accommodated by the addition of a Archimedean buoyance terms, which are present in any accelerated frame of reference. From the viewpoint of force balance, Rosenberg *et al.* [5] introduced the effective cross-sectional areas of the rigid rod and its mushroom front end to the modified Bernoulli equation. Based on this modification, and estimating the target resistance from the expansion of a cylindrical cavity in an infinite medium, they claimed good agreement between the model and experimental data. On the other hand, Wright [6, 7] and Wright and Frank [8] questioned the validity of the

assumption of the steady state and the estimate of the interface pressure by the modified Bernoulli equation. Lately, Anderson and Walker [9] have made a further examination of Tate's model with the aid of numerical simulation. They indicated that because a finite region of the projectile deceleration is not accounted for, Tate's model predicts the rear of the projectile decelerates too late and too rapidly at the end of penetration. On the basis of discrepancies in the prediction between Tate's model and numerical simulation, Walker and Anderson [10] proposed a nonsteady state penetration model. Anderson *et al.* [11, 12] also reported that target resistance varies considerably during penetration and that the resistance value used in Tate's model should be considered as an average value to give the correct penetration depth. Recently, Grace [13] proposed a new one-dimensional theory of non-steady penetration of long rods into semi-infinite targets. In his model, the target is modeled as a finite mass that resides within the semi-infinite target and undergoes erosion and deceleration during the penetration process. Based on Newton's law, deriving the equations of motion for the target and the penetrator leads to a new  $u-v$  relationship that has replaced the modified Bernoulli equation.

Evidently, there are some deficiencies in the theory of Tate and Alekseevskii in spite of the fact that it has been broadly thought of as a standard reference for one-dimensional long-rod penetration over the past decades. Indicating the fact that this model does not consider mass transfer into the plastic zone and a non-zero mushroom strain at the penetrator tip, Jones *et al.* [14] used the impulse-momentum equation to modify Tate's equation of motion for the undeformed section:

$$l\dot{v} + \dot{l}(v - u) = -\frac{P_B}{\rho(1 + e)} \quad (1)$$

where  $l$  is current length of the undeformed penetrator, of which the current velocity is  $v$ , and  $u$  is the penetration velocity of the penetrator tip. The parameter  $\rho$  represents the rod density and  $e$  is the mushroom strain, which is assumed constant throughout the quasi-steady state. The term  $P_B$  is the penetrator/target interface pressure, estimated by the modified Bernoulli equation. In this equation, the relative velocity term at the left hand side provides the contribution to momentum due to mass transfer into the plastic zone and the strain factor  $e$  reflects the mushrooming effect at the tip of the penetrator. Compared with Eqn (1), Tate's model has assumed the plastic region is instantaneously consumed, which renders no change in momentum and a 0% compressive strain. Although Eqn (1) can characterize the penetration process in more detail, the pressure term based on the modified Bernoulli equation is ad-hoc. It is apparent that the pressure used by Tate, which in effect causes a 0% compressive strain to the penetrator tip, must be too high for a penetrator with a non-zero mushroom strain. Therefore, Cinnamon *et al.* [15] tried to reduce the net force by introducing a factor to account for the variation of the pressure across the mushroom face. This factor is further correlated to the target strength. With this factor  $n$  added, Eqn (1) becomes

$$l\dot{v} + \dot{l}(v - u) = -\frac{P_B}{\rho(1 + n)(1 + e)}. \quad (2)$$

Accompanied with an initial transient analysis and a linear relationship between crater volume and kinetic energy, reasonable predictions can be obtained for impact velocities from 1 km/s to 3 km/s. However, an attempt to integrate the equations analytically and piece together the initial transient and quasi-steady state motions does not succeed due to the presence of a singularity. Consequently, Cinnamon [16] made a further analysis in which the average pressure at quasi-steady state is assumed constant over the range of impact velocities for particular shot combinations. The average pressure is again correlated to the target strength. A similar attempt to integrate these equations analytically by replacing the modified Bernoulli pressure  $P_B$  in Eqn (1) with the average pressure also cannot be accomplished due to the presence of a singularity. The reason for this may be the answer for the unsuccessful implementation of modified pressure laws in the model. This suggests that

a reconstruction of the  $u-v$  relationship may be necessary in this model, and that a more accurate pressure law may depend on more than densities and strengths.

In this paper, the model proposed by Jones *et al.* [14] is re-examined. Based on the work of Wang and Jones [17], the original equation of motion will be decomposed into two parts to account for the motions of the mushroom region and the undeformed portion of the penetrator separately. As a result of incorporating these two equations with the kinematic equation derived by Wilson *et al.* [18], a new pressure law is proposed to replace the modified Bernoulli equation. This new estimate for pressure, taking the effect of mushroom strain in the penetrator tip into account, leads to a new interpretation of the interaction between the pressure and the penetrator during penetration.

Two different cases are considered to implement the pressure law in the model and reasonable agreement with experimental data is achieved with each. In the first case, the pressure is assumed velocity independent (constant) and a new  $u-v$  relationship is constructed. Direct integration of this system leads to a closed form solution for the penetration depth. The constant pressures are obtained by matching the penetration depths and then further correlated to the target strengths. In the second case, a velocity-dependent pressure with a shape factor is considered. Numerical integration is required to obtain the penetration depths. The shape factor, which was first proposed by Alekseevskii without physical interpretation, is also correlated to mushroom strain. With these considerations, the previous singularity problem is removed and reasonably accurate predictions can be achieved.

#### DEVELOPMENT: A NEW PRESSURE LAW

Although Eqn (1) contains the motions of the mushroomed tip and the undeformed (rigid) part of the penetrator, its validity is undermined when the force (pressure) that controls deceleration is incorrectly assumed. The equations of motion are separately derived for the mushroom and the undeformed portions of the penetrator, as illustrated in Fig. 1. From the free body diagram of the mushroom, the equation of motion over the time  $t$  to  $t + \Delta t$  is obtained from Newton's 2nd law:

$$\rho(-\Delta l A_0) \left[ \frac{u-v}{\Delta t} \right] = \sigma A - \sigma_0 A_0. \quad (3)$$

The ratio in the bracket represents the acceleration of the mushroom over  $\Delta t$ . The area of the

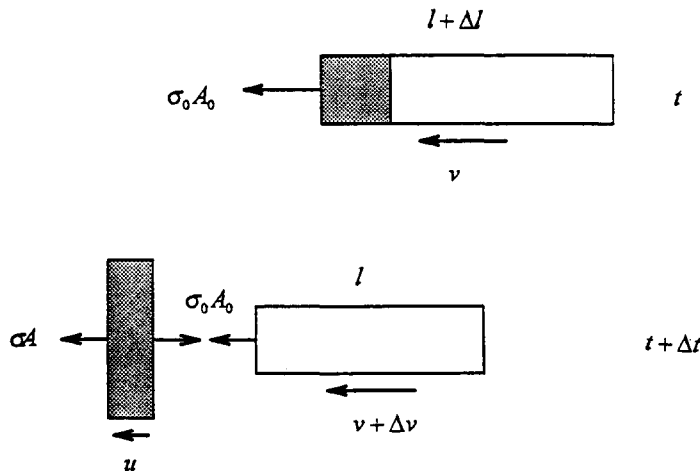


Fig. 1. Free body diagrams of the undeformed and mushroom head (shaded area) of a rod during the time interval  $\Delta t$ .

fully developed mushroom,  $A$ , and the area of the original penetrator,  $A_0$ , can be correlated to the engineering strain  $e$ :

$$e = \frac{A_0}{A} - 1. \quad (4)$$

Accordingly, let  $\Delta t$  approach zero and use Eqn (4), and Eqn (3) becomes

$$\rho l(v - u) = \frac{\sigma}{1 + e} - \sigma_0. \quad (5)$$

Similarly, from the free body diagram of the undeformed section, the equation of motion has the form:

$$\rho A_0 l \frac{\Delta v}{\Delta t} = \sigma_0 A_0 \quad (6)$$

and let  $\Delta t$  approach zero, the Eqn (6) becomes

$$\rho l \dot{v} = \sigma_0. \quad (7)$$

Note that  $\sigma$  is the penetrator/target interface stress and  $\sigma_0$  is the internal stress exerted between the plastic region and undeformed portion of the penetrator. Both of these two stresses are time-dependent in nature. Note that if we combine Eqn (5) and (7) by eliminating the term  $\sigma_0$ , the resulting equation is exactly the same as Eqn (1). Moreover, Eqn (7) is actually the equation of motion used by Tate [2], if we assume that  $\sigma_0$  is the dynamic yield stress for the penetrator.

Now, we introduce the kinematic relationship derived by Wilson *et al.* [18], which has the form:

$$e \dot{l} = v - u. \quad (8)$$

By eliminating  $\dot{l}$  term between Eqn (5) and (8) and solving for  $\sigma$ , we arrive at an expression for the target/penetrator interface stress (pressure):

$$P = -(1 + e) \left[ \frac{\rho(v - u)^2}{e} + \sigma_0 \right] \quad (9)$$

where  $\sigma$  has been replaced by  $P$  and the negative sign denotes compression. Before we make further use of Eqn (9) to solve a penetration problem, more insight into this equation should first be made. If we compare Eqn (9) with the modified Bernoulli equation used by Tate [2], the dimensionless coefficient of the term  $(v - u)^2$ ,  $-(1 + e)/e$ , in Eqn (9) is more general than  $1/2$ . The so-called shape factor proposed by Alekseevskii [1] can be reflected by this coefficient as well. It should be clear that the mushroom strain influences the interface pressure.

### A PENETRATION MODEL BASED ON CONSTANT PRESSURE

Based on Eqns (7–9), a new penetration model can be established once an estimate for  $P$  has been found. To begin, we assume that the target/penetrator interface pressure is approximately constant throughout the steady state. Actually, this assumption dates back to the early eighteenth century work of Robins and Euler [19]. However, it is only applicable to the penetration of nondeforming projectiles at low velocities [19, 20]. Considering the penetration of deforming penetrators, Christman and Gehring [21] used this assumption to typify steady state penetration. The validity of this assumption has also been discussed by Anderson *et al.* [9, 12] using a numerical simulation. Based on the constant pressure, the  $u$ – $v$  relationship is thus obtained directly from Eqn (9) in terms of  $P$ :

$$u = v - \left[ \frac{1}{\rho} \left( \frac{-e_1}{1 + e_1} P - e_1 \sigma_0 \right) \right]^{1/2} \quad (10)$$

where  $e$  has been replaced by  $e_1$ , which denotes the constant strain during quasi-steady state

penetration. Accordingly, the difference between the penetration velocity  $u$  and the current velocity  $v$  is also constant. Now, we incorporate Eqns (7) and (8) to obtain

$$\int_V^0 (v - u) dv = \frac{\sigma_0 e_1}{\rho} \int_{L_0}^{l_f} \frac{dl}{l} \quad (11)$$

where  $V$  is the initial impact velocity and  $l_f$  is the residual length of the undeformed section at the end of the steady-state phase. Because the difference between  $u$  and  $v$  is a constant, a direct integration of Eqn (11) gives

$$l_f = L_0 \exp\left(-\frac{K\rho V}{e_1\sigma_0}\right) \quad (12)$$

where  $K = v - u = \text{constant}$ , which comes from Eqn (10). By assuming that a final transient phase adds little to total penetration, the total steady-state penetration depth  $z$  at  $u = 0$  can now be obtained by evaluating the integral:

$$z = \int u dt = \int \frac{u}{v} dv = \frac{\rho}{\sigma_0} \int_V^K (v - K) l dv. \quad (13)$$

After integration, a closed form solution for  $z$  can be found:

$$z = -\frac{\rho L_0}{a^2 \sigma_0} [\exp(a(K - V)) + (aV - aK - 1)] \quad (14)$$

where  $a = \rho K / \sigma_0 e_1$  is a constant. It should be noted that  $\sigma_0$  represents the dynamic yield strength of the penetrator, which is treated as an empirical constant. At this point, the remaining problem is how to find  $P$ .

#### *Determining the constant pressure*

One straightforward way to determine the constant pressure is to find the pressure that can best match the experimental data for penetration depth. The mushroom strain is obtained from the experimental data of crater diameters. It is noted that the current model does not explicitly account for the influence of the target strength factor ( $R$ ) but that of the penetrator's dynamic yield strength  $\sigma_0$ . According to Anderson *et al.* [11], the penetration performance is more susceptible to the target strength than the penetrator strength. Consequently, it is anticipated that these  $P$  values may be correlated to target strengths. After investigating the experimental data, only the  $P$  values that best fit the penetration depths at low velocities (1 km/s–2 km/s) were obtained. Moreover, it is found that the value of  $P$  in each case is approximately twice the dynamic yield strength of the target. However, at higher velocities, this  $P$ – $R$  relationship underestimates penetration performance. Conceptually, this can be understood from the impulse–momentum equation that develops the model. This approach relates the time-dependent (or velocity-dependent) penetration force to the product of a constant pressure and impact velocity-dependent mushroom strain (or area). At low impact velocities, the increasing force can be approximately reflected by the product because of increasing mushroom area, when impact velocity increases. However, as the impact velocity gets higher, the mushroom area is approaching some asymptotic limit [15], so the product cannot keep up with the increasing trend of the force. This accounts for the limitation of the application of constant pressure at lower velocities. On the other hand, for low-aspect-ratio penetrators, because a quasi-steady state penetration process may be very short, or may not even be reached, the assumptions of quasi-steady state and constant pressure are not appropriate. Besides, the dynamic yield strengths of some soft targets (like 1100-O AL and lead) are usually very strain-rate sensitive at higher strain rates [22, 23], so a constant value for  $R$  is not appropriate. Based on these considerations, the constant pressure model has been mainly used to investigate the cases involving aspect ratios greater than 10 and steel targets.

#### *Prediction based on the constant pressure*

A huge database of penetration mechanics compiled by Anderson *et al.* [24] has been used to examine the validity of the proposed models in this paper. The predictions based on

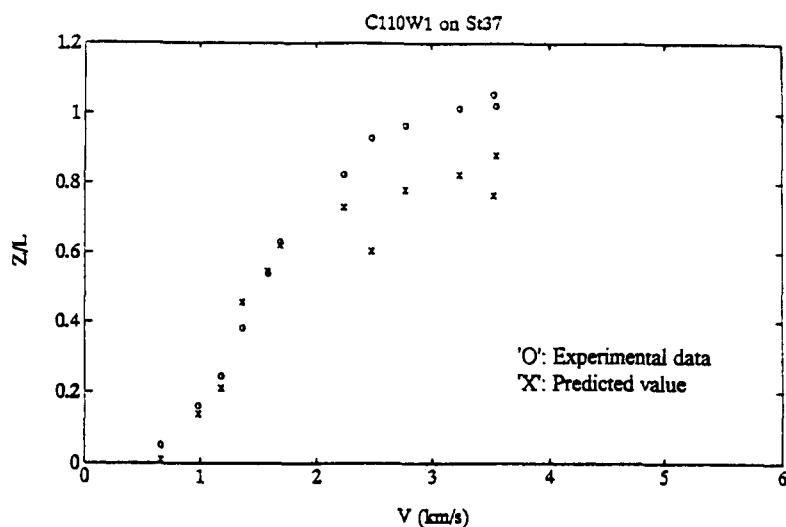


Fig. 2. Normalized penetration depth ( $Z/L$ ) vs impact velocity ( $V$ ).

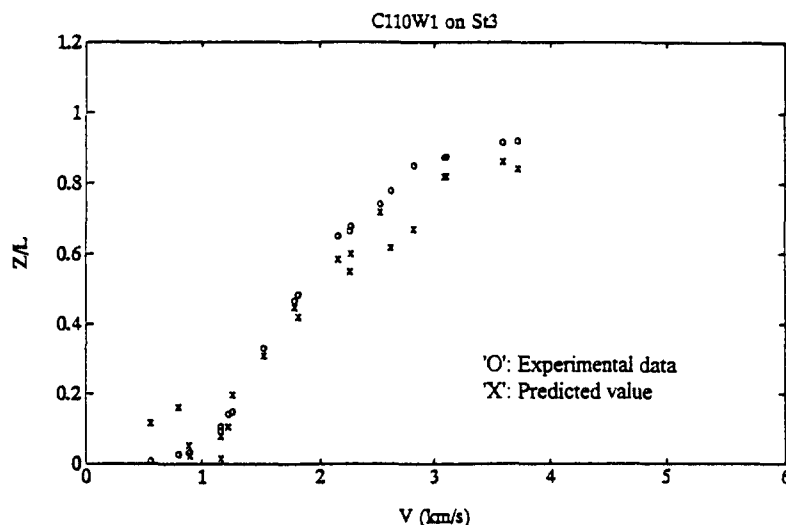


Fig. 3. Normalized penetration depth ( $Z/L$ ) vs impact velocity ( $V$ ).

constant pressure show common S-shaped penetration curves. For the cases involving steels against steels (e.g. Figs 2–4) and tungsten alloys against steels (e.g. Figs 5 and 6), the theoretical predictions (crosses) can reasonably match the experimental observations (circles) at velocities between 1 km/s and 2 km/s, but suffer considerable error when the velocities exceed 2 km/s. In addition to the previously stated limitation at low velocities, it is possibly due to inertia effects which become more significant relative to strength effects at higher velocities. Numerical simulation also shows that the magnitude of the nonsteady state of penetration increases with impact velocity, and that it contributes significantly to the total penetration at the higher impact velocities [12]. Thus, a velocity-dependent pressure will be invoked to cure the deficiency in the current model. The uncertainties in the experimental data of crater sizes apparently can cause some scattered predictions. For the cases investigated, realistic estimates for material strengths ( $\sigma_0$  or  $R$ ) have been used: C110W1–1200 MPa, St37–860 MPa, St52–960 MPa, St3–1300 MPa, D17–1600 MPa, and W8–1800 MPa.

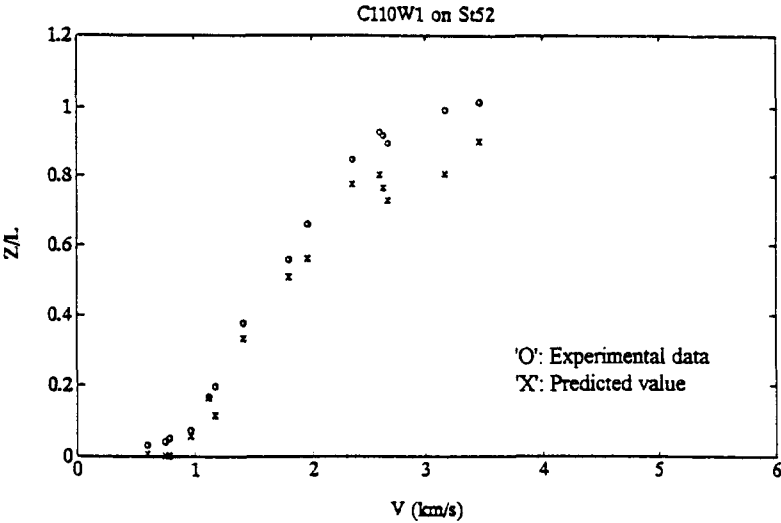


Fig. 4. Normalized penetration depth ( $Z/L$ ) vs impact velocity ( $V$ ).

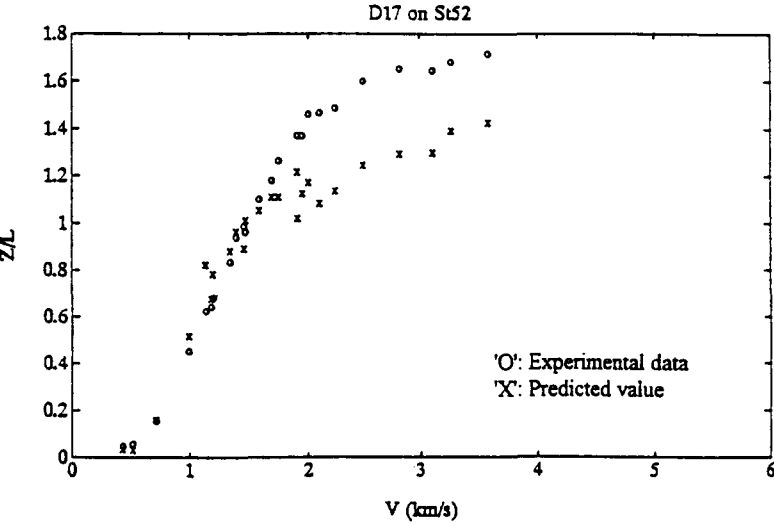


Fig. 5. Normalized penetration depth ( $Z/L$ ) vs impact velocity ( $V$ ).

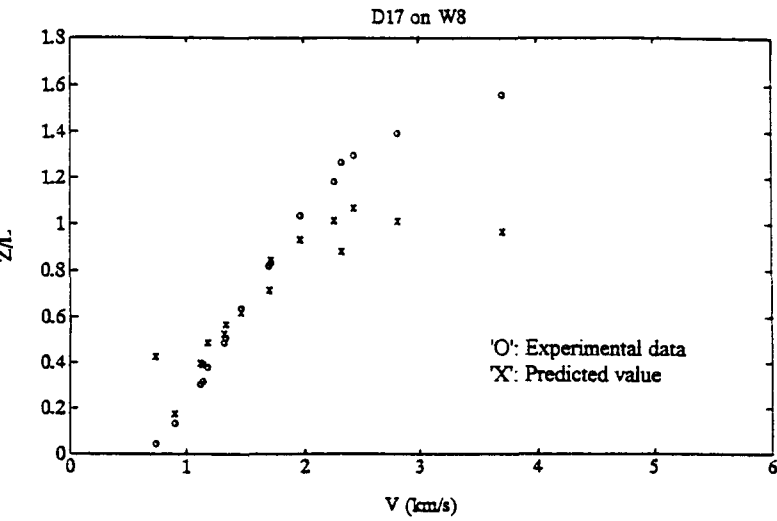


Fig. 6. Normalized penetration depth ( $Z/L$ ) vs impact velocity ( $V$ ).

## A PENETRATION MODEL BASED ON VELOCITY-DEPENDENT PRESSURE

As the constant-pressure model has indicated, the accuracy of the prediction is reasonably good at low impact velocities ( $< 2$  km/s) for long rods. The predicted S-shaped trend does not match well in the high velocity range ( $\geq 2$  km/s). In addition to inertia effects at higher velocities, the interface pressure may change with the deformation at the penetrator tip (mushroom strain) and penetration velocities. The assumption of constant pressure throughout the quasi-steady state cannot account for these factors. Motivated by these observations, a velocity-dependent pressure is considered to modify the previous elementary pressure estimate.

### Shape factor

Although Eqn (9) has represented the interface pressure  $P$  in terms of the current penetration velocity  $u$  and current undeformed section velocity  $v$ , one more equation is needed to construct the relationship between  $u$  and  $v$  if  $P$  is velocity-dependent. Let's recall the theory proposed by Alekseevskii [1], who considers the pressure balance across the target/penetrator interface and postulates the following equation:

$$Y + k_p \rho_p (v - u)^2 = R + k_t \rho_t u^2 \quad (15)$$

where  $k_p$  and  $k_t$  are shape factors that characterize the deformed regions in the penetrator and target materials, respectively.  $Y$  and  $R$  represent the dynamic strength of the penetrator and target, respectively. Simply indicating that these two shape factors depend on the flow geometry and assuming that they are approximately 1/2 based on the hydrodynamic model, Alekseevskii does not give any further physical insight into these factors. Swanson and Donaldson [25] proposed a so-called integral theory of impact to model the long rod penetration process. In their model, they assume the target/penetrator interface pressure is governed by fluid drag,  $C_d$ , and the adiabatic hardness. The adiabatic hardness is used to explain the strength factor for the target and is defined as the product of the target density,  $\rho_t$ , and the energy per unit mass dissipated in the form of plastic work as the target flows around the penetrator,  $E_t^*$ . Thus, the interface pressure assumes the following form:

$$P = \rho_t \left( \frac{C_d}{2} u^2 + E_t^* \right) \quad (16)$$

where  $u$  is penetration velocity. It is not difficult to find that the dimensionless drag factor  $C_d$  in Eqn (16) plays a very similar role to the shape factor  $k_t$  in Eqn (15). Lately, Rosenberg *et al.* [5] considered the equilibrium of force at rod/target interface by introducing effective cross-sectional areas of the rigid rod and its mushroomed front end to the modified Bernoulli equation. The resultant area ratio, which was specifically taken as two in their model, is somewhat like the shape factor mentioned by Alekseevskii [1]. On the other hand, the coefficient  $-(1 + e_1)/e_1$  in Eqn (9) has also revealed the possible physical meaning of the shape factor  $k_p$  in Eqn (15). Based on the above overview of the shape factor, it is reasonable to assume that the pressure has the form:

$$P = k_t \rho_t u^2 + R = -(1 + e_1) \left[ \frac{\rho(v - u)^2}{e_1} + \sigma_0 \right] \quad (17)$$

where  $k_t$  is a constant and will be determined later.  $R$  represents the dynamic yield strength of the target, which for example, can be determined by a Taylor impact test. Equation (17) thus establishes a new  $u-v$  relationship. Particularly, if  $k_t$  and  $-(1 + e_1)/e_1$  are both set equal to 1/2, then Eqn (17) returns the modified Bernoulli equation. Or, in other words, the modified Bernoulli equation is a special case of Eqn (17) when  $e_1 = -2/3$  and the penetrator's strength ( $Y$ ) is one third of its dynamic yield strength. It is interesting to note that  $e_1 = -2/3$  is the critical value of the tip strain in the earlier penetration theory of Jones *et al.* [14], which was further elaborated by Gillis *et al.* [26].

### Derivation of the model

A new penetration model based on velocity-dependent interface pressure can be developed by incorporating Eqn (7), (8), and (17). For the sake of convenience, we rewrite Eqn (17) as

$$P = k_1 u^2 + R = k_2 (v - u)^2 + Y \quad (18)$$

where

$$k_1 = k_t \rho,$$

$$k_2 = -\left(\frac{1 + e_1}{e_1}\right) \rho_p,$$

and

$$Y = -(1 + e_1) \sigma_0.$$

Note that  $\sigma_0$  is negative because it is a compressive stress. From Eqn (18), we can rearrange and get a quadratic equation in  $u$ :

$$(k_1 + k_2)u^2 + 2k_2vu + (k_3 - k_2v^2) = 0 \quad (19)$$

where  $k_3 = R - Y$ . A further solution for  $u$  depends on the sign of the coefficient  $(k_1 - k_2)$ . By letting  $\zeta^2 = k_1/k_2$ ,  $u$  can be written in the following form:

$$u = \frac{v - \zeta[v^2 - A]^{1/2}}{1 - \zeta^2} \quad (20)$$

for  $k_1 \neq k_2$ , and  $A = \frac{k_3}{k_1}(1 - \zeta^2)$ , or

$$u = \frac{k_2v^2 - k_3}{2k_2v} \quad (21)$$

for  $k_1 = k_2$ . Based on Eqns (20) and (21), the residual length of the penetrator can be obtained by evaluating the integral in Eqn (11). Consequently, the residual penetrator length has the form:

$$\frac{l}{L_0} = \left[ \frac{v + \sqrt{v^2 + A}}{V + \sqrt{V^2 + A}} \right]^{\rho A \zeta / 2 e_1 \sigma_0 (1 - \zeta^2)}$$

$$\times \exp \left[ \frac{\rho \zeta}{2 e_1 \sigma_0 (1 - \zeta^2)} [(v \sqrt{v^2 + A} - \zeta v^2) - (V \sqrt{V^2 + A} - \zeta V^2)] \right] \quad (22)$$

for  $k_1 \neq k_2$ , or

$$\frac{l}{L_0} = \exp \left[ \frac{\rho}{4 e_1 \sigma_0} (v^2 - V^2) \right] \left[ \frac{v}{V} \right]^{\rho k_3 / 2 k_2 e_1 \sigma_0} \quad (23)$$

for  $k_1 = k_2$ . Now, the penetration depth  $z$  can be obtained by solving

$$z = \int u dt = \int \frac{u}{v} dv = \frac{\rho}{\sigma_0} \int u dv \quad (24)$$

which is similar to Eqn (13). A numerical integration is required to evaluate the integral in Eqn (24).

According to Tate's theory [27], there exists a critical velocity during the deceleration of the penetrator, below which rigid body penetration will continue if  $Y > R$  and a further erosion of the penetrator without gaining penetration depth will continue if  $Y < R$ . A similar consideration can be made for the current model.

I. *Rigid body penetration.* This implies  $v = u$  and  $l$  is constant, so we can solve for the critical velocity  $v_c$  from Eqn (18):

$$v_c = \left[ \frac{Y - R}{k_1} \right]^{1/2}. \quad (25)$$

Because the penetrator remains rigid in this stage, the interface pressure should be the stress responsible for decelerating the residual penetrator (with mushroom tip and constant length). Hence, we transform Eqn (7) to

$$\rho_p l_c \dot{v} = -(k_1 v^2 + R) \quad (26)$$

where  $l_c$  represents the residual length that corresponds to  $v = v_c$ , and can be found from either Eqn (22) or Eqn (23). Integrating Eqn (24) by using Eqn (26), the penetration depth during this stage is obtained:

$$z_c = \frac{\rho_p l_c}{2k_1} \ln \left[ \frac{k_1 v_c^2 + R}{R} \right]. \quad (27)$$

Thus, when  $T > R$ , the total penetration depth is equal to the sum of Eqns (24) and (27).

II. *Erosion without penetration.* This implies  $u = 0$ , so we can solve for the critical velocity  $v_c$  from Eqn (18):

$$v_c = \left[ \frac{R - Y}{k_2} \right]^{1/2}. \quad (28)$$

In this stage, the interface pressure is not high enough to make the target material deform, but high enough to continue the material flow across the rigid–fluid interface of the penetrator. Therefore, the undeformed section of the penetrator is decelerated by its dynamic yield strength. That is, Eqn (7) is still valid. Accompanied with Eqn (8) ( $u = 0$ ), Eqn (7) can be integrated to give the final length:

$$l_f = l_c \exp \left[ -\frac{\rho v_c^2}{2e_1 \sigma_0} \right]. \quad (29)$$

From the previous discussion, it is likely that most of the penetration problems fall in the second type, erosion without penetration. This is because the strength factor of penetrator ( $Y$ ) is reduced by the factor  $-(1 + e_1)$ . This implies that at the end of penetration, once  $v < v_c$ , the second type of penetration is the most likely case. Up to this point, we have established a new penetration model based on a new pressure law, but the shape factor  $k_t$  is still unknown.

#### Determining the shape factor

In order to investigate the behavior of the shape factor, we find its value for each shot by matching the experimental depth data. Motivated by the previous observation that the shape factor  $k_p$  is a function of  $e_1$ , we make the same assumption for  $k_t$ . After examining all the cases, a common trend can be found:

$$\begin{aligned} k_t(e_1) &\rightarrow \infty & \text{when } e_1 &\rightarrow e_0 \\ k_t(e_1) &\rightarrow 0 & \text{when } e_1 &\rightarrow -1 \end{aligned} \quad (30)$$

where  $e_0$  and  $k_0$  are both constants. This relation implies that the shape factor becomes large when the mushroom strain approaches some constant (at low velocities) and approaches a small constant value when the mushroom strain approaches  $-1$  (at high velocities). From another viewpoint, this relation is also conceptually similar to the definition of the drag coefficient. Based on Eqn (30), the hyperbolic-type property of  $k_t(e_1)$  can be approximated by taking the first three terms of a power series of the form:  $\sum_{n=0}^{\infty} c_n (e_1 - e_0)^{-n}$ . That is,

$$k_t \cong c_0 + \frac{c_1}{(e_1 - e_0)} + \frac{c_2}{(e_1 - e_0)^2} \quad (31)$$

where  $c_0$ ,  $c_1$ , and  $c_2$  are constants to be determined after a value of  $e_0$  has been assumed. For most of the cases,  $e_0$  is chosen to comply with  $k_t = 0$  when  $e_1 = -1$ . That is,  $k_0$  in Eqn (30) is normally zero. In only one case, "AL alloy on lead", has  $k_t$  been non-zero as  $e_1$  approaches  $-1$ . In such cases, a maximum trend for the penetration curve can be obtained. On the other hand, it is also found that for most high-aspect-ratio ( $L/D \geq 10$ ) cases,  $c_0$  can be simply set equal to zero. The exceptions to this are the low-aspect-ratio cases ( $L/D = 3$ ), "1100-O AL on 1100-O AL" and "C1015 steel on C1015 steel". In these cases,  $c_0$  has a significant contribution in determining  $k_t$ . However, a further attempt to find regularities among these three constants, or to correlate these constants to other physical parameters, is difficult due to many untractable uncertainties in material properties.

#### Prediction based on velocity-dependent pressure

By using the strains predicted by the initial transient analysis from Wang and Jones [28], the current model is again tested with a large volume of experimental data. Some selected results predicted by the model, compared with the experimental data, have been presented graphically in the form of normalized penetration depth ( $Z/L$ ) vs impact velocity ( $V$ ). The predicted results agree well with the experimental data over an impact velocity range of 0–4 km/s. The S-shaped curve is also reasonably well reflected by the model.

As Fig. 7 shows for the case of aluminum alloy penetrators against lead targets ( $L/D = 10$ ,  $\sigma_0 = 275$  MPa, and  $R = 60$  MPa), the current model can successfully show the maximum trend of penetration performance, which cannot be achieved in some of our previous work. Figure 8 shows reasonable agreement throughout the whole impact velocity range for the case of D17 WA against St52 steel targets ( $L/D = 10$ ,  $\sigma_0 = 1600$  MPa, and  $R = 960$  MPa). As to the cases of C1015 steel on C1015 steel ( $L/D = 3$ ,  $\sigma_0 = R = 650$  MPa) and 1100-O AL on 1100-O AL ( $L/D = 3$ ,  $\sigma_0 = R = 160$  MPa) shown in Figs 9 and 10 respectively, the increasing trends to  $Z/L$  at higher velocities ( $V > 2$  km/s), which cannot be captured by our previous models [4, 16], can now be accurately predicted by the current model.

## CONCLUSION

In this paper, an attempt has been made to modify the modified Bernoulli equation used by Tate. By decomposing the equation of motion proposed by Jones *et al.* [14] into two parts, a new analytical form for the interface pressure has been developed. This pressure form is more general than the modified Bernoulli equation because the mushroom strain effect is included. As a first approximation, a constant interface pressure ( $P$ ) was assumed dominant through the quasi-steady state, which gives a new relation between the current tail and the

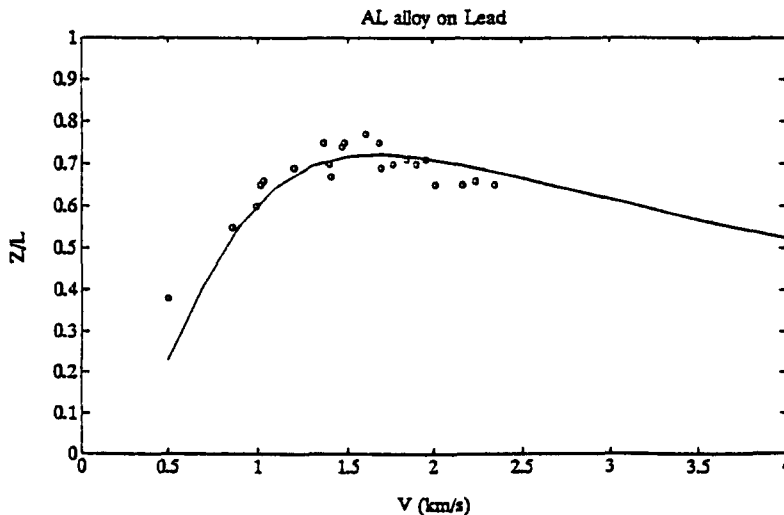


Fig. 7. Normalized penetration depth ( $Z/L$ ) vs impact velocity ( $V$ ).

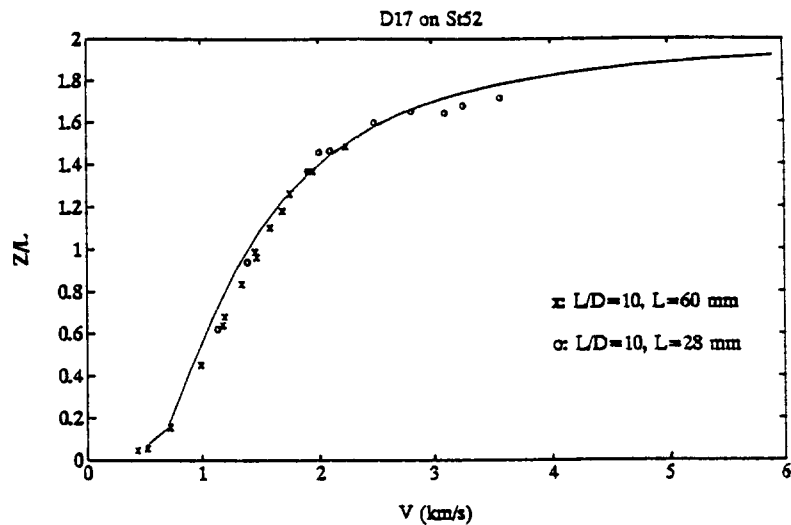


Fig. 8. Normalized penetration depth ( $Z/L$ ) vs impact velocity ( $V$ ).

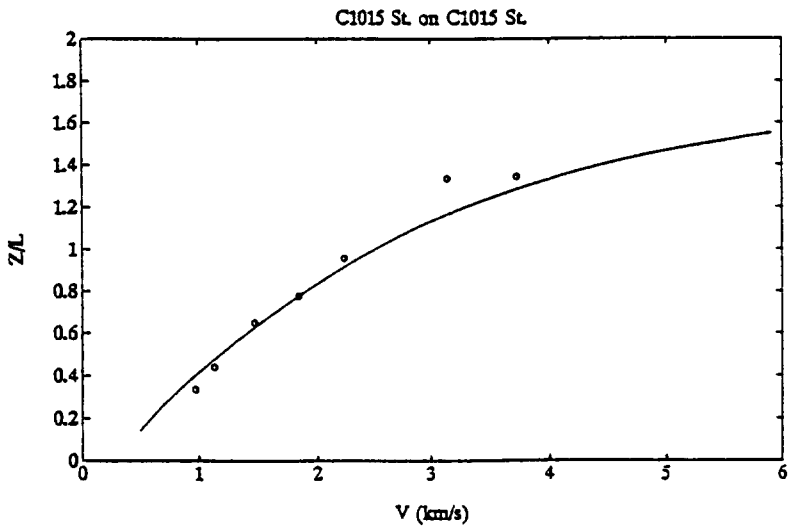


Fig. 9. Normalized penetration depth ( $Z/L$ ) vs impact velocity ( $V$ ).

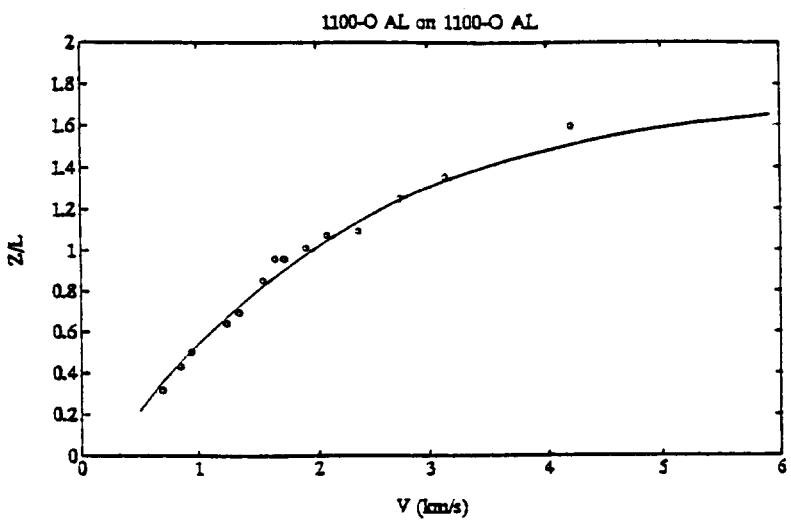


Fig. 10. Normalized penetration depth ( $Z/L$ ) vs impact velocity ( $V$ ).

penetration velocity [Eqn (10)]. By employing the experimental strains,  $P$  for each case is found and is approximately twice of  $R$ . Based on this constant pressure, the model can be integrated analytically and a closed-form solution for penetration is obtained. This removes the singularity problem that has often prevented the integration of the equations of motion introduced by Jones *et al.* [14]. However, the predicted penetration depths show reasonable agreement only in cases with low impact velocities and large aspect ratio. Moreover, most of these cases involve WA or steel penetrators against steel targets. For the penetrations at higher velocities, a constant  $P$ – $R$  relationship may lose effectiveness because the effect of inertia and the contribution of nonsteady state penetration become more significant. Accordingly, the pressure distribution may be more velocity-dependent. Despite these disadvantages, the constant-pressure model reveals a promising direction for the construction of a new pressure law.

Motivated by the constant-pressure model, a velocity-dependent pressure law was formulated. The new pressure law is suggested by equating the previously developed pressure from the viewpoint of the penetrator to an assumed pressure with a similar structure from the viewpoint of the target. By recalling the original theory proposed by Alekseevskii [1], the obscure “shape factor” was reconsidered and identified in terms of the new pressure law. From the viewpoint of the penetrator, the shape factor is a function of the mushroom strain, but from the viewpoint of the target, the shape factor ( $k_t$ ) cannot be obtained *a priori* and has to be determined by examining the experimental data. All the distributions of  $k_t$  vs the strain were commonly hyperbolic, which can be approximated by an inverse power series expansion with respect to the strain. Nevertheless, further effort failed to correlate the coefficients of the series to known physical parameters. However, with the shape factor added to the model, the system can be integrated numerically without any singularity problem.

This model gives a more accurate prediction than the constant-pressure model, as long as the shape factor is properly chosen and a correct strain trend is determined. It is noteworthy that the velocity-dependent pressure enables the model to capture the maximum trend of the penetration curves for soft targets, which has invalidated some of the previous models. For penetrations by low-aspect-ratio penetrators, better agreement can be achieved because the shape factor probably has offset the deficiency of the assumption of quasi-steady state by taking the flow geometry at the penetrator/target interface into account.

Finally, as a comparison with the numerical simulation made by Anderson *et al.* [12], by choosing an average mushroom strain of  $-0.8$ , the pressure predicted by the velocity-independent model is plotted as a function of impact velocity for the shot combination of D17 on W8 [24] in Fig. 11. The increasing trend of pressure with impact velocity is generally consistent with the observation from numerical simulation when  $e$  is constant. On the other

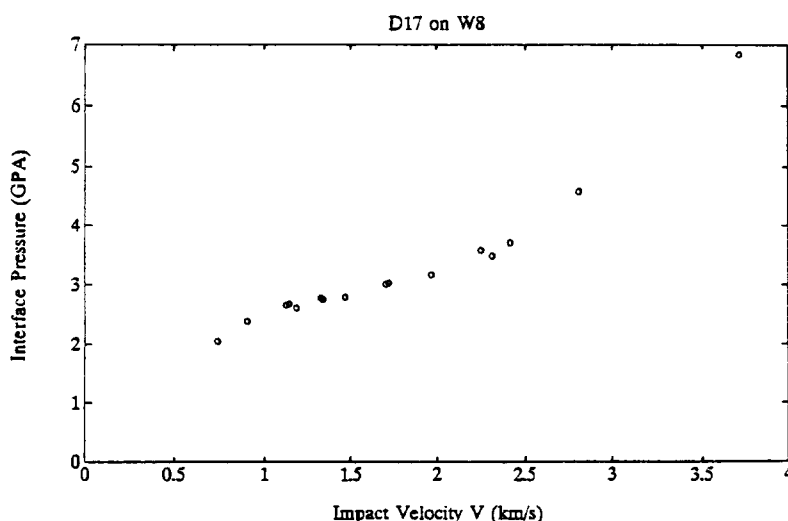


Fig. 11. Interface pressure ( $P$ ) predicted by velocity-independent model vs impact velocity ( $V$ ).

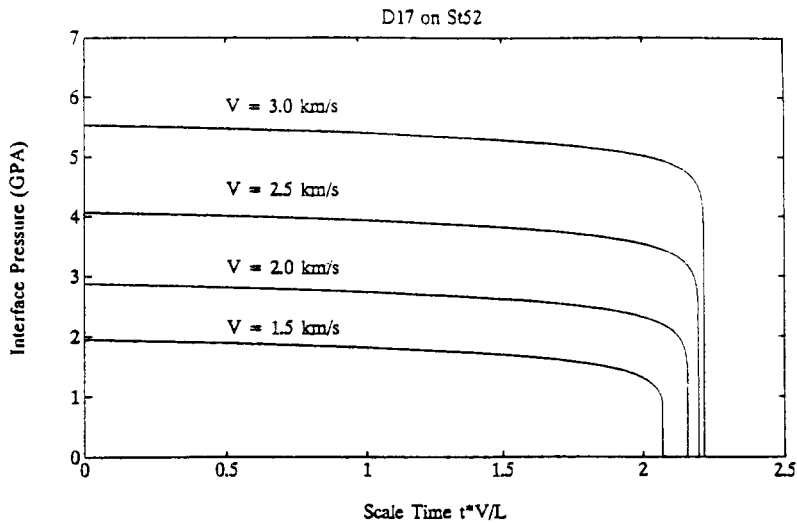


Fig. 12. Interface pressure ( $P$ ) predicted by velocity-dependent model vs scale time ( $tV/L$ ).

hand, the pressure predicted by the velocity-dependent model is plotted as a function of scaled time for the shot combination of D17 on St52 [24] in Fig. 12. By choosing an average mushroom strain of  $-0.8$  and four typical impact velocities, similar to those used by Anderson *et al.* [12], similar increasing trends of pressure with impact velocity are obtained. However, the predicted pressure is apparently much lower than that obtained from the numerical simulation. This is due to the increase in area at the penetrator tip. A compressive strain  $-0.8$  is the equivalent to increasing the diameter by a factor of 2.24.

## REFERENCES

1. V. P. Alekseevskii, Penetration of a rod into a target at high velocity. *Combustion, Explosion, and Shock Waves* **2**, 63–66 (1966).
2. A. Tate, A theory for the deceleration of long rods after impact. *J. Mech. Phys. Solids* **15**, 387–399 (1967).
3. A. Tate, Long rod penetration models—Part I. A flow field model for high speed long rod penetration. *Int. J. Mech. Sci.* **28**, 353–548 (1986).
4. A. Tate, Long rod penetration models—Part II. Extensions to the hydrodynamic theory of penetration. *Int. J. Mech. Sci.* **28**, 599–612 (1986).
5. Z. Rosenberg, E. Marmor and M. Mayseless, On the hydrodynamic theory of long-rod penetration. *Int. J. Impact Engng* **10**, 483–486 (1990).
6. T. W. Wright, Penetration with long rods: a theoretical framework and comparison with instrumented impacts. ARBRL-TR-02323, U.S. Army Ballistic Research Laboratory, Aberdeen Proving Ground, MD (1981).
7. T. W. Wright, A survey of penetration mechanics for long rods. In *Computational Aspects of Penetration Mechanics* (Edited by J. Chandra and J. E. Flaherty), *Lecture Notes in Engineering*, pp. 85–196. Springer-Verlag, Berlin-Heidelberg (1983).
8. T. W. Wright and K. Frank, Approaches to penetration problems. In *Impact: Effects of Fast, Transient Loadings* (Edited by W. J. Amman, W. K. Liu, J. A. Studer and T. Zimmermann). A. A. Balkema, Rotterdam (1988).
9. C. E. Anderson and J. D. Walker, An examination of long-rod penetration. *Int. J. Impact Engng* **4**, 481–501 (1991).
10. J. D. Walker and C. E. Anderson, A nonsteady-state model for penetration. *Proc. 13th Int. Symp. on Ballistics*, Stockholm, Sweden (1992).
11. C. E. Anderson, J. D. Walker and G. E. Hauver, Target resistance for long-rod penetration into semi-infinite targets. *Nucl. Engng Design* **138**, 93–104 (1992).
12. C. E. Anderson, D. L. Littlefield and J. D. Walker, Long-rod penetration, target resistance, and hypervelocity impact. *Int. J. Impact Engng* **14**, 1–12 (1993).
13. F. I. Grace, Nonsteady penetration of long rods into semi-infinite targets. *Int. J. Impact Engng* **14**, 303–314 (1993).
14. S. E. Jones, P. P. Gillis and J. C. Foster, Jr., On the penetration of semi-infinite targets by long rods. *J. Mech. Phys. Solids* **35**, 121–131 (1987).
15. J. D. Cinnamon, S. E. Jones, J. W. House and L. L. Wilson, A one-dimensional analysis of rod penetration. *Int. J. Impact Engng* **12**, 145–166 (1992).
16. J. D. Cinnamon, Further one-dimensional analysis of long-rod penetration of semi-infinite targets. Master's Thesis, The University of Texas at Austin (1992).
17. P. Wang and S. E. Jones, An elementary theory of one-dimensional rod penetration using a new estimate for pressure, (Abstract). *Proc. Annual Meeting of the Society of Engineering Science*, College Station, Texas, October (1994).

18. L. L. Wilson, J. C. Foster, S. E. Jones and P. P. Gillis, Experimental rod impact results. *Int. J. Impact Engng* **8**, 15–25 (1989).
19. W. Johnson, *Impact Strength of Materials*, pp. 306. Edward Arnold, London (1972).
20. J. S. Rinehart and J. Pearson, *Behavior of Metals under Impulsive Loads*, pp. 199–200. The American Society for Metals, Cleveland Ohio (1954).
21. D. R. Christman and J. W. Gehring, Analysis of high-velocity projectile penetration mechanics. *J. Appl. Phys.* **37**, 1579–1587 (1966).
22. U. S. Lindholm, Some experiments with the split Hopkinson pressure bar. *J. Mech. Phys. Solids* **12**, 317–335 (1964).
23. U. S. Lindholm and L. M. Yeakley, High strain-rate testing: tension and compression. *Exp. Mech.* **8**, 1–9 (1968).
24. C. E. Anderson, B. L. Morris and D. L. Littlefield, A penetration mechanics database. SWRI Report 3593/001, Southwest Research Institute, San Antonio, TX (1992).
25. C. V. Swanson and C. duP. Donaldson, Application of the integral impact theory to modeling long-rod penetrators. Aeronautical Research Associates of Princeton, ARAP Report 333 (1978).
26. P. P. Gillis, S. E. Jones, L. L. Wilson and J. C. Foster, An analytical and experimental approach to the penetration of semi-infinite targets by long rods. In *Recent Advances in Impact Dynamics of Engineering Structures*, ASME-AMD-Vol. 105 (Edited by D. Hui and N. Jones) (1989).
27. A. Tate, Further results in the theory of long rod penetration. *J. Mech. Phys. Solids* **17**, 141–150 (1969).
28. P. Wang and S. E. Jones, An analysis of one-dimensional penetration using a revised estimate for impulse. *SECTAM XVII Conf.*, Hot Springs National Park, Arkansas, April 10–12 (1994).